Interaction of Spin-Labeled Nucleotides with Sarcoplasmic Reticulum Adenosinetriphosphatase†

Celia R. G. Oliveira,‡ Carol Coan,*,§ and Sergio Verjovski-Almeida‡

Departamento de Bioquimica, Instituto de Ciencias Biomedicas, Universidade Federal do Rio de Janeiro, Rio de Janeiro, Brazil, and Department of Physiology, University of the Pacific School of Dentistry, San Francisco, California 94115

Received December 1, 1987; Revised Manuscript Received April 14, 1988

ABSTRACT: Spin-labeled derivatives of AMP-PCP, ATP, and 2′-deoxy-ATP, with a nitroxide moiety attached to the ribose ring [3′-*O*-(1-oxy-2,2,5,5-tetramethylpyrroline-3-carbonyl)nucleotide], are used to study the nucleotide binding site stoichiometry of sarcoplasmic reticulum (SR) ATPase. With all derivatives, a maximal binding of 4.5 nmol/mg of SR protein is found, a value close to the number of phosphorylation sites obtained with ATP. The spin-labeled nucleotides cannot be utilized by the enzyme as substrates. Binding of spin-labeled nucleotides is inhibited by labeling the ATPase with fluorescein 5′-isothiocyanate, indicating that all the labeled nucleotide is located at the catalytic site. Additions of spin-labeled ATP to vesicle suspensions during steady turnover demonstrate competitive inhibition of both catalysis and the regulatory effect normally exhibited by ATP. As secondary binding of spin-labeled ATP is not detected at pertinent concentrations, it is suggested that both functions of ATP may be effected through a single site.

It has been established for some time that the sarcoplasmic reticulum (SR)[1] ATPase shows biphasic kinetics when the velocity of hydrolysis is measured as a function of ATP concentration (Inesi et al., 1967; Yamamoto & Tonomura, 1967). However, while the velocity increases with millimolar additions of ATP, both the coupling ratio (two Ca^{2+} transported per ATP hydrolized) and the steady-state level of phosphoenzyme intermediate remain the same (Verjovski-Almeida & Inesi, 1979). Basically two types of mechanisms have been proposed to explain the ATP-induced increase in velocity: one in which ATP binds to a second, independent site to modulate the hydrolysis mechanism (Verjovski-Almeida & Inesi, 1979; Dupont, 1977; Taylor & Hatten, 1979; Moller et al., 1980; Coll & Murphy, 1986) and an another in which ATP rebinds with lower affinity to the catalytic site following the release of ADP and causes an increase in rate of intermediate steps in the cycle (Neet & Green, 1977; McIntosh & Boyer, 1983; Cable et al., 1985; Gould et al., 1986; Bishop et al., 1987).

One reason that controversy on this point remains, after an extended period of experimental observation, is the lack of a good means for determining the binding stoichiometry of ATP to the enzyme at high ATP concentrations. As a means of approaching this question, we have prepared spin-labeled (SL) derivatives of AMP-PCP, ATP, and 2′-deoxy-ATP with the spin moiety attached to the ribose ring. A specific advantage of a spin probe in this type of study is the large dependence of spectral parameters on the tumbling rate of the probe, allowing for a clear separation of bound probe from free probe in the EPR spectrum. This, in turn, allows us to monitor the fraction of the probe bound to the enzyme directly, in solution, at high probe concentration. The bound SL-nucleotide–ATPase spectrum can then be resolved and integrated to determine the binding stoichiometry without further assumptions.

Materials and Methods

SR vesicles were prepared from the white skeletal muscle of rabbit hind legs by using methods previously described (Elter & Inesi, 1972). Vesicles were stored in a buffered sucrose medium (30% sucrose/10 mM MOPS, pH 6.8) at 4 °C and were used within 4–5 days of preparation. 2,2,5,5-tetramethyl-3-pyrroline-3-carboxylic acid was purchased from Molecular Probes. ATP, AMP-PCP [adenosine 5′-(β,γ-methylenetriphosphate)], 2′-deoxy-ATP, *N*-(1-oxy-2,2,6,6-tetramethyl-4-piperidinyl)iodoacetamide (ISL), and 1,1′-carbonyldiimidazole were purchased from Sigma.

Protein concentrations were measured according to the techniques of Lowry et al. (1951), using bovine serum albumin as a standard. ATPase activity was monitored by using a coupled assay system with pyruvate kinase (40 μg/mL), PEP (1 mM), lactic acid dehydrogenase (120 μg/mL), and NADH (10 μg/mL) (Anderson & Murphy, 1983). The reaction medium contained 10 mM $MgCl_2$, 2 mM EGTA, 2 mM $CaCl_2$, 100 mM MOPS, pH 6.8, 80 mM KCl, 1 μg/mL ionophore A23187, and approximately 10 μg/mL SR. To determine competitive inhibition at the catalytic site, a series of enzyme activities were measured at nonsaturating ATP concentrations with sequential additions of spin-label nucleotides. The data were either analyzed in the form of a Dixon plot or fit directly with a nonlinear regression algorithm, or both. To determine competitive inhibition concomitantly at the catalytic site and the regulatory site, sequential additions of Mg·ATP were made to a solution containing a given concentration of SL-ATP. The full concentration range was obtained by overlapping points from given experiments where the ATP concentration was varied from 0.1 μM to 20 mM. Titration data were fit to a multisite binding scheme with a computer program incorporating a nonlinear regression algorithm (Bevington, 1969) for a set of parameters which best described all titration data. Corrections were made for basal activity by repeating the ATP titrations, at each SL-ATP concentration, in the presence of 10 mM EGTA. To check the hydrolysis of SL-ATP by the ATPase without the coupling system present, the rate of P_i production was measured by

† Supported by CNPq/FINEP (Brazil) (to C.R.G.O. and S.V.-A.), NIH Grant HL 27867-01 (to C.C.), and an American Heart Association grant-in-aid with funds contributed in part by the Florida Affiliate (to C.C.).

‡ Universidade Federal do Rio de Janeiro.

§ University of the Pacific School of Dentistry.

[1] Abbreviations: SR, sarcoplasmic reticulum; AMP-PCP, adenosine 5′-(β,γ-methylenetriphosphate); EGTA, ethylene glycol bis(β-aminoethyl ether)-*N*,*N*,*N*′,*N*′-tetraacetic acid; FITC, fluorescein isothiocyanate (isomer I); MES, 2-(*N*-morpholino)ethanesulfonic acid; MOPS, 3-(*N*-morpholino)propanesulfonic acid; PEP, phosphoenolpyruvate.

0006-2960/88/0427-5923$01.50/0

using a molybdate quench according to the methods of Murphy (1981). Levels of steady-state phosphoenzyme intermediate were determined by incubation with [^{32}P]ATP, followed by filtration, according to the methods of Anderson et al. (1984). FITC-SR was prepared by incubating 7 nmol of FITC/mg of SR protein in pH 6.8 buffer (100 mM MOPS/80 mM KCl) for 12 h at 4 °C. ATPase activity was checked to ensure complete inhibition.

Synthesis of SL-AMP-PCP, SL-ATP, and SL-2′-Deoxy-ATP. A modified method of Jeng and Guillory (1975) was used to prepare the 2′/3′-*O*-(1-oxy-2,2,5,5-tetramethyl-pyrroline-3-carbonyl) derivative of the nucleotide, where 2′/3′ denotes an isomeric mixture, referred to here simply as SL-nucleotide. Dry *N*,*N*′-carbonyldiimidazole was mixed with an equal concentration of 2,2,5,5-tetramethyl-3-carboxy-1-pyrroline-1-oxyl in anhydrous DMF at room temperature. After overnight incubation, water was removed, and the nucleotide was precipitated from a 1:1 mixture of anhydrous ether and methanol (6 mL). A second precipitation step recovered additional labeled nucleotide.

The combined precipitate was dried under N_2, dissolved in 100–200 μL of H_2O, and spotted on silica gel (250-μm) TLC plates which were chromatographed in isobutyric acid/0.5 N NH_3 (5:3) for 7–8 h. The labeled nucleotides were clearly separated from traces of starting materials and exhibited a major band with an R_f value close to that reported for SL-ATP (Jeng & Guillory, 1975), and two minor bands with R_f values close to those reported for SL-ADP and SL-AMP. The major band was removed and added to 6 mL of 100 mM MES buffer (pH 6), and the silica gel was homogenized to form a slurry. The suspension was incubated on ice for 10 min, and the SL-nucleotides were recovered from the supernatant following high-speed centrifugation.

EPR Measurements. To prepare samples for EPR measurements, aliquots of concentrated solutions of SL-AMP-PCP, $CaCl_2$, $MgCl_2$, EDTA, or EGTA were added, as required, to 80/mg mL SR to given a final volume of approximately 50 μL and 65–75 mg/mL SR. An EPR sample cell with a removable plug was made from quartz tubing with calibration marks so that the tube could be oriented in the field and the sample centered in the cavity.

An IBM-Bruker ER-200D EPR spectrometer (X band) interfaced with an IBM S-9001 computer and with an ER-4111VT variable-temperature control system was used with IBM EPR Application software (version 2) for all experimental measurements and data analysis. A field modulation of 100 kHz and microwave power of 19.9 mW were used in all cases; other conditions varied with the requirements of a given measurement. When line heights were used to obtain binding stoichiometries, a modulation amplitude of 0.6 G was used with a response time of 80 ms and a sweep time of 200 s. The spectrum was scanned repeatedly to ensure stability with time, i.e., that the spin-label was stable in the given solution, the SL-nucleotide was not being hydrolyzed by the ATPase, or the degree of binding to the ATPase changing in any way. Once a spectrum of the SL-nucleotide–SR solution had been obtained, the sample cell was removed, 1 μL of 500 mM AMP-PCP injected into the cell, and the spectrum scanned a second time. Following measurement, the protein concentration was determined for each sample. The binding stoichiometry was then calculated from $\{[1 + h/(h + [\text{AMP-PCP}])][(v + 1)/v][\text{SL-AMP-PCP}]\}/(\text{mg/mL SR protein})$ where v is the sample volume and h is the peak to peak line height of the isotropic signal generated by the free label. Calculated values were independent of the spectral line used for measurement. Controls were run to determine if additions of 1 μL of AMP-PCP affected the line height of the free SL-nucleotide per se. Under conditions used here, a measurable change in line height was not observed when AMP-PCP was added either to an aqueous solution of SL-nucleotide (no SR) or to an FITC-SR suspension in which nucleotide binding had been inhibited.[2]

When spectra were obtained for purposes of subtraction, a modulation width of 2.5 G was frequently used, as this gave a better resolution of the bound component, and the slight overmodulation of the free signal did not affect our ability to eliminate it by subtraction. Spectra were time-averaged for 15–20 min in order to increase the signal to noise ratio. The spectra were aligned, and the free SL-AMP-PCP (the spectrum after AMP-PCP addition) was subtraced in increments of 1% until the free component could be reduced no further without the introduction of artifacts into the bound SL-AMP-PCP spectrum. These artifacts arise when the spectra are not perfectly aligned or when the line widths vary slightly. The fact that the apparent "free signal" could never be completely eliminated indicates that there were still some very small changes in line widths on the addition of 1 μL of AMP-PCP. This could be due to small changes in either collisional broadening or viscosity.

Double integrations of the resolved bound component spectrum were normalized to integrations of the complete SL-AMP-PCP spectrum (bound + free component) to determine the concentration of the bound SL-AMP-PCP. Corrections were made for the residual free signal by using the line height ratio of this component to the total free signal to estimate the apparent concentration. Ultimately, the magnitude of the residual free signal became the limiting factor in obtaining an accurate concentration for the bound component, due primarily to the subtraction artifacts inherent in this signal.

Results and Discussion

An EPR spectrum of SL-AMP-PCP in the presence of a vesicular suspension of SR is given in Figure 1. The isotropic signal of the free label appears as three sharp bands. This free label is in equilibrium with the fraction of label which is bound to the enzyme, and as the gain is increased, the low- and high-field extrema of the highly immobilized bound component become apparent in the spectrum. The introduction of a small aliquot of cncentrated AMP-PCP then causes the signal of the free label to increase while the bound component is eliminated from the spectrum, indicating that the excess of AMP-PCP has replaced the SL-AMP-PCP at binding sites on the enzyme.

The two sets of spectra can be subtracted to resolve the spectrum of the bound component, as shown in Figure 2. Double integration of this spectrum then provides binding stoichiometry. The contribution of the small, residual free signal to the integral was subtracted as described under Materials and Methods. This contribution was very small over most of the titration curve (i.e., 3–5% at 2 mM, 10–15% at 6 mM). Alternatively, the line height increase in the signal of the free SL-AMP-PCP on the addition of AMP-PCP (Figure 1) can be used to calculate binding stoichiometries. Line height increases give fairly accurate estimations of stoichiometries when the SL-AMP-PCP concentration is close to the site concentration of the ATPase. However, in the

[2] At low total ionic strength, changes in line height can be observed on addition of concentrated AMP-PCP due to changes in the degree of collisional broadening of the spin probe.

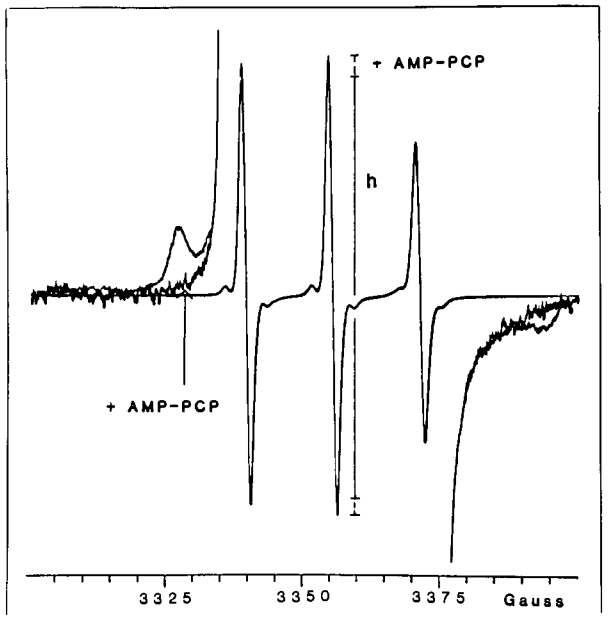

FIGURE 1: EPR spectrum of 2 mM SL-AMP-PCP with SR ATPase. The signal generated by the bound spin-label is visible on the extrema of the isotropic free label signal when the gain is increased by 2 orders of magnitude. On the addition of 10 mM AMP-PCP, the line height of the isotropic signal increases by 10%, and the bound component is eliminated from the spectrum. Conditions: 65 mg/mL SR; 10 mM $MgCl_2$; 10 mM $CaCl_2$; 10 mM EGTA; 80 mM KCl; 100 MOPS, pH 6.8; 25 °C.

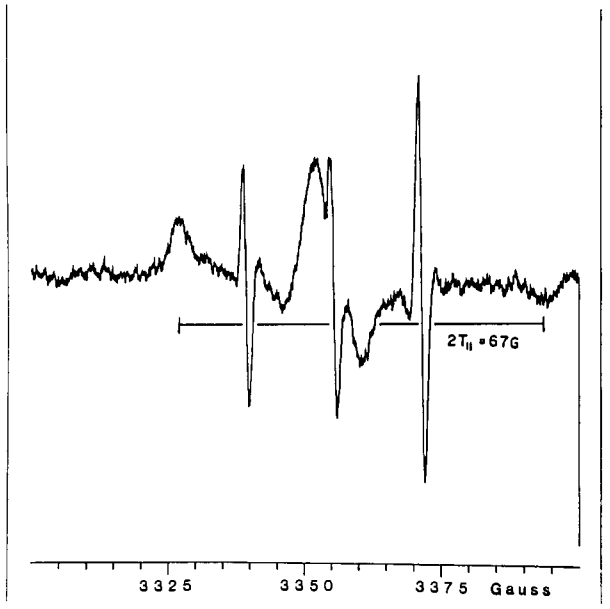

FIGURE 2: Resolved signal of SL-AMP-PCP·ATPase, obtained by the subtraction of the free SL-AMP-PCP signal (the spectrum after the addition of AMP-PCP) from the spectrum shown in Figure 1.

millimolar range, the fraction of label bound to the enzyme becomes increasingly small, and above 6 mM, the line height increase falls within the range of experimental reproducibility.

A titration curve using both methods to determine the binding stoichiometry is given in Figure 3. It is evident in the figure that 4–5 nmol of SL-AMP-PCP/mg of SR protein was bound to the ATPase in the concentration range studied. Titrations with either SL-2′-deoxy-ATP (Figure 3, open triangles) or SL-ATP (closed triangles) showed essentially the same profile. Although SL-ATP hydrolysis could not be detected by normal means, there was a small loss in the bound SL-ATP signal with time when concentrations of SL·ATP which were close to the site concentration of the ATPase were

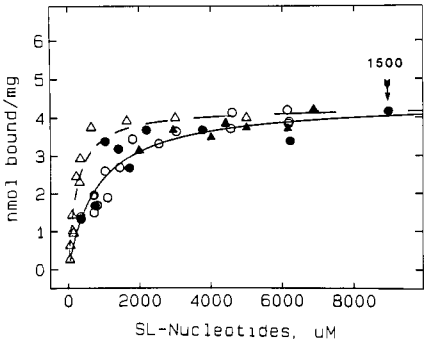

FIGURE 3: Titration of SR ATPase by SL-nucleotides. Bound SL-AMP-PCP from line height measurements (○) and from spectral integrations (●); bound SL-2′-deoxy-ATP from line heights (△); bound SL-ATP from spectral integrations (▲). Conditions: SR, 65–75 mg/mL; 10 mM $MgCl_2$; 10 mM $CaCl_2$; 10 mM EGTA; 80 mM KCl; 100 mM MOPS, pH 6.8; 25 °C. The solid line gives the best fit to the SL-AMP-PCP data and the dashed line to the SL-2′-deoxy-ATP data. Binding parameters obtained by the fit are given in the text.

used, and we could not obtain the low end of the titration curve. It should be noted that at the enzyme concentrations required in EPR experiments, even an extremely low level of basal activity could account for this, as the SL-ATP must be held in a 1:1 complex with the enzyme for an extended period of time with no breakdown of the complex to time-average the signal.

We routinely find in our preparations that about 4 nmol/mg of E–P can be formed from ATP, and it appears that the SL-nucleotides may bind exclusively to the catalytic site. It is also important to note that we only measure the SL-nucleotide that is released when AMP-PCP, which is known to be a strong competitive inhibitor of ATP, is added to the solution and that all the bound component is eliminated on this addition. In turn, this eliminates the possibility that the bound signal is generated from nonspecific sites, as would be observed if the nitroxide moiety were interacting with a unique site on the enzyme, or that the change in line height is due to the partitioning of the label into the membrane.

To further substantiate the preferential binding of SL-nucleotide to the catalytic site, binding studies were repeated with FITC-ATPase, as it is well established that under controlled conditions FITC will selectively label a lysyl residue near the catalytic site of the ATPase and prevent nucleotide binding (Pick & Karlish, 1980; Anderson et al., 1982; Highsmith & Murphy, 1984). We see no evidence of SL-nucleotide binding to the FITC-ATPase. Furthermore, these experiments allowed us to check our assumption that the isotropic line heights were not changing on the introduction of small aliquots of AMP-PCP per se.

When the binding curves are fit with a simple binding equation, values of K_d and $[E{\cdot}S]_{max}$ which give the best fit can be determined. For SL-AMP·PCP, this K_d was 821 ± 150 μM and for SL-2′-deoxy-ATP, 233 ± 46 μM, higher than values reported for AMP-PCP and 2′-deoxy-ATP (90 μM, Coll & Murphy, 1986; and 17 μM, Anderson & Murphy, 1985, respectively). Both sets of binding data predicted an $[E{\cdot}S]_{max}$ of 4.5 ± 0.2 μmol/mg. Although direct binding measurements could not be made with SL-ATP in the range where a K_d could be determined, we could determine the K_i of SL-ATP in the range of ATP concentrations where binding is expected to take place only at the catalytic site (1–3 μM ATP). SL-ATP (0–200 μM) showed a competitive inhibition pattern, and a linear Dixon plot gave a K_i of 150 μM. A direct fitting of the data gave a K_i of 127 μM and accurately predicted ATP binding parameters.

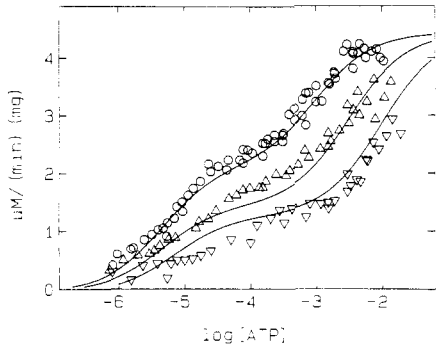

FIGURE 4: Velocity of ATP hydrolysis as a function of ATP concentration in the presence of 260 μM SL-ATP (△) and 520 μM SL-ATP (▽) and in the absence of SL-ATP (○). Solid lines give the fit generated by the best set of parameters which can describe all three titration curves. Description of the fitting techniques and values for the parameters are given in the text.

Although very stable to hydrolysis, it is clear that SL-AMP·PCP has a considerably reduced affinity for the ATPase, while SL-2′-deoxy-ATP and SL-ATP have affinities which should make them more competitive with ATP. The nitroxide moiety has been reported to isomerize rapidly between the 2′- and 3′-positions on the ribose of SL-ATP (Crowder & Cooke, 1987). Comparison of SL-2′-deoxy-ATP binding data with those of SL-ATP indicates that localization of the spin moiety on the 3′-position does not significantly alter the binding properties.

Binding curves were repeated with SL-AMP-PCP at pH 6.0 and 7 and in the presence of EDTA which should have removed both endogenous Ca^{2+} and Mg^{2+}. We did not find variations in the binding affinity which could be detected by our techniques under any of these conditions. Variation in ATP binding and AMP-PCP binding as a function of pH and Mg^{2+} concentration has been reported (Dupont et al., 1985; Coll & Murphy, 1986), and it is quite possible that modification of the ribose ring by the nitroxide moiety tends to minimize these variations. Also, there was no apparent difference in the resolved SL-AMP-PCP·ATPase spectra under any of these conditions.

A question central to the role of ATP in regulating the hydrolysis mechanism concerns the existence of a second site. While it is apparent here that SL-nucleotides bind only to the catalytic site, it is not clear from these binding data alone that a second site does not exist. It is possible that binding to a putative regulatory site would not be observed if changes in SL-nucleotide affinity for this site were even higher than for the catalytic site. In fact, other types of substrate analogues which have a lower affinity for the catalytic site (ITP, GTP, acetyl phosphate) also have a decreased ability to activate turnover of the enzyme cycle (de Meis & de Mello, 1973). To resolve this question, we have pursued a series of competitive inhibition experiments to determine the ability of SL-ATP to interact with the enzyme at both sites from a functional standpoint.

A titration of the velocity of ATP hydrolysis over the ATP concentration range needed to saturate both the catalytic and the regulatory functions is shown in Figure 4. ATP was added as a Mg·ATP complex to hold the free Mg^{2+} concentration constant, and an ATP-regenerating system was used. This titration was then repeated in the presence of 260 and 520 μM SL-ATP. For these experiments, SL-ATP was chosen because the K_i would predict the most favorable competition with ATP.

It is very clear in Figure 4 that the enzyme velocity is inhibited over the concentration range required both to saturate the catalytic site and to fully effect enzyme regulation. The three sets of titration data were best fit by a set of equations describing competition between ATP and SL-ATP for both functions with $K_i(1) = 117 \pm 40$ μM and $K_i(2) = 121 \pm 30$ μM, respectively (Figure 4). In addition, fitting procedures predicted appropriate parameters for ATP [$K_m(1) = 4.4$ μM, $K_m(2) = 1000$ μM, $V_m(1) = 2.0$ μmol mg^{-1} min^{-1}, and $V_m(2) = 4.5$ μmol mg^{-1} min^{-1}]. However, to obtain the best quality fit, it was also necessary to take into consideration $V_m(3)$, the effect of SL-ATP acting in a regulatory capacity during the catalysis of ATP. The best fit was given by a $V_m(3) = 1.2$ nmol mg^{-1} min^{-1}. As this is lower than the maximal velocity in the absence of regulation [$V_m(1) = 2.2$ μmol mg^{-1} min^{-1}], it predicts a degree of inhibition, rather than activation, for SL-ATP as a regulatory agent. The goodness of the fit was indicated by a standard deviation (taken from the square root of the variance between the calculated and measured velocities for all three curves) of 10%.

It is not obvious from inspection alone that the observed inhibition could not be accounted for by extended effects of SL-ATP inhibition at the catalytic site. However, when $K_i(2)$ was eliminated in fitting procedures, the generated curves could not describe the biphasic nature of the titration data, reasonable parameters for ATP could not predicted when fit in conjunction with the inhibition data, and the standard deviation was large (25%).

CONCLUSIONS

It is very clear from the data presented here that SL-AMP-PCP, SL-2′-deoxy-ATP, and SL-ATP have a binding stoichiometry to the SR ATPase of approximately 4.5 nmol/mg of SR protein, even at very high spin-label concentrations. However, it is also apparent that SL-ATP competitively inhibits both the catalysis of ATP and the regulation of enzyme turnover observed at high ATP concentrations. As the best estimate of K_i for the site associated with regulation (121 μM) is 2 orders of magnitude lower than concentrations where binding data can be obtained, it is further apparent that a separate regulatory site is not available to bind SL-ATP when the enzyme is not turning over.

To reasonably account for the inhibition data obtained with SL-ATP, no assumptions needed to be made about the relation between the catalytic and regulatory sites nor the steps in the enzyme cycle associated with regulation, and the fitting procedures could adequately describe a model in which ATP rebinds with lower affinity to the catalytic site at an intermediate step in the cycle to effect regulation, or one in which a separate regulatory site becomes exposed only after enzyme phosphorylation. Neither of these possibilities can be eliminated by the SL-nucleotide binding data alone. The latter model would be more in accord with the studies of Coll and Murphy (1986) on the noncompetitive inhibition of ADP. However, Bishop and co-workers (Bishop et al., 1987) have been able to titrate the ATPase phosphoenzyme intermediate directly with TNP-AMP in a concentration range where inhibition of the regulatory effect was observed and found evidence for only one binding site. Given the results of Bishop and co-workers, only a model in which a single site is responsible for both catalysis and regulation can account for the combined experimental data. This model is also supported by the kinetic analysis of AMP-PCP inhibition performed by Cable and co-workers (Cable et al., 1985). The recent rapid kinetic analysis of ATP binding properties by Lacapere and Guillain (1988) as well as previous studies by Nakamura and co-workers (Nakamura et al., 1986), and by Champeil and Guillain (1986), indicates that regulation is most likely to be associated with steps following enzyme phosphorylation but

preceding Ca^{2+} release into the lumen of the vesicles.

ACKNOWLEDGMENTS

We thank Rudene DiCarlo for her expert technical assistance and Dr. Alexander J. Murphy for the use of his computer programs to fit nonlinear regression algorithms to binding data.

REFERENCES

Anderson, J. P., Moller, J. V., & Jorgensen, P. L. (1982) *J. Biol. Chem. 257*, 8300–8307.
Anderson, K. W., & Murphy, A. J. (1983) *J. Biol. Chem. 258*, 14276–14278.
Anderson, K. W., Coll, R. J., & Murphy, A. J. (1984) *J. Biol. Chem. 259*, 11487–11490.
Bevington, P. R. (1969) *Data Reduction and Error Analysis for the Physical Sciences*, McGraw-Hill, New York.
Bishop, J. E., Al-Shawi, M. K., & Inesi, G. (1987) *Biochemistry 26*, 4650–4663.
Cable, M. B., Feher, J. J., & Briggs, F. N. (1985) *Biochemistry 24*, 5612–5619.
Champeil, P., & Guillain, F. (1986) *Biochemistry 25*, 7623–7633.
Coll, R. J., & Murphy, A. J. (1985) *FEBS Lett. 187*, 131–134.
Coll, R. J., & Murphy, A. J. (1986) *Biochem. Biophys. Res. Commun. 138*, 652–658.
Crowder, M. S., & Cooke, R. (1987) *J. Biophys. Soc. 51*, 323–333.
de Meis, L., & de Mello, M. C. (1973) *J. Biol. Chem. 248*, 3691–3701.
Dupont, Y. (1977) *Eur. J. Biochem. 72*, 185–190.
Dupont, Y., Pugeois, R., Ronjat, M., & Verjovski-Almeida, S. (1985) *J. Biol. Chem. 260*, 7241–7249.
Elter, S., & Inesi, G. (1972) *Biochim. Biophys. Acta 282*, 174–179.
Gould, G. W., East, J. M., Froud, R. J., McWhirter, J. M., Stefanova, H. I., & Lee, A. G. (1986) *Biochem. J. 237*, 217–227.
Highsmith, S., & Murphy, A. J. (1984) *J. Biol. Chem. 259*, 14651–14656.
Inesi, G., Goodman, J. J., & Watanabe, S. (1967) *J. Biol. Chem. 242*, 4637–4643.
Jeng, S. J., & Guillory, R. J. (1975) *J. Supramol. Struct. 3*, 448–468.
Lacapere, J. J., & Guillain, F. (1988) *Biophys. J. 53*, 338a.
Lowry, O., Roebrough, N., Farr, A., & Randall, R. (1951) *J. Biol. Chem. 193*, 265–275.
McIntosh, D. B., & Boyer, P. D. (1983) *Biochemistry 22*, 2867–2875.
Moller, J. V., Lind, K. E., & Andersen, J. P. (1980) *J. Biol. Chem. 255*, 1912–1920.
Murphy, A. J. (1981) *J. Biol. Chem. 256*, 12046–12050.
Nakamura, Y., Kurzmack, M., & Inesi, G. (1986) *J. Biol. Chem. 261*, 3090–3097.
Neet, K. E., & Green, N. M. (1977) *Arch. Biochem. Biophys. 178*, 588–597.
Pick, U., & Karlish, S. J. D. (1980) *Biochim. Biophys. Acta 626*, 255–261.
Taylor, J. S., & Hatten, D. (1979) *J. Biol. Chem. 254*, 4402–4407.
Verjovski-Almeida, S., & Inesi, G. (1979) *J. Biol. Chem. 254*, 18–21.
Yamamoto, T., & Tonamura, Y. (1967) *J. Biochem. (Tokyo) 62*, 558–575.

Isotope Effect Studies of the Pyridoxal 5′-Phosphate Dependent Histidine Decarboxylase from *Morganella morganii*†

Lynn M. Abell and Marion H. O'Leary*
Departments of Chemistry and Biochemistry, University of Wisconsin—Madison, Madison, Wisconsin 53706
Received December 22, 1987; Revised Manuscript Received April 12, 1988

ABSTRACT: The pyridoxal 5′-phosphate dependent histidine decarboxylase from *Morganella morganii* shows a nitrogen isotope effect $k^{14}/k^{15} = 0.9770 \pm 0.0021$, a carbon isotope effect $k^{12}/k^{13} = 1.0308 \pm 0.0006$, and a carbon isotope effect for L-[α-^{2}H]histidine of 1.0333 ± 0.0001 at pH 6.3, 37 °C. These results indicate that the overall decarboxylation rate is limited jointly by the rate of Schiff base interchange and by the rate of decarboxylation. Although the observed isotope effects are quite different from those for the analogous glutamate decarboxylase from *Escherichia coli* [Abell, L. M., & O'Leary, M. H. (1988) *Biochemistry 27*, 3325], the intrinsic isotope effects for the two enzymes are essentially the same. The difference in observed isotope effects occurs because of a roughly twofold difference in the partitioning of the pyridoxal 5′-phosphate–substrate Schiff base between decarboxylation and Schiff base interchange. The observed nitrogen isotope effect requires that the imine nitrogen in this Schiff base is protonated. Comparison of carbon isotope effects for deuteriated and undeuteriated substrates reveals that the deuterium isotope effect on the decarboxylation step is about 1.20; thus, in the transition state for the decarboxylation step, the carbon–carbon bond is about two-thirds broken.

Pyridoxal 5′-phosphate (PLP)[1] is the coenzyme for the majority of amino acid decarboxylases. The general mechanism by which these enzymes operate is well understood (Scheme I), and many aspects of this mechanism have been studied (Boeker & Snell, 1972). A smaller class of amino acid decarboxylases lack PLP but contain instead a covalently

† This work was supported by Grants PCM 8216597 and DMB 8517501 from the National Science Foundation.

[1] Abbreviations: PLP, pyridoxal 5′-phosphate; HEPES, *N*-(2-hydroxyethyl)piperazine-*N*′-2-ethanesulfonic acid; MES, 2-(*N*-morpholino)ethanesulfonic acid; CHES, 3-(cyclohexylamino)ethanesulfonic acid.

0006-2960/88/0427-5927$01.50/0